Electron emission mechanism during the nanosecond high-voltage pulsed discharge in pressurized air

D. Levko,[a] S. Yatom, V. Vekselman, and Ya. E. Krasik
Department of Physics, Technion, 32000 Haifa, Israel

(Received 30 December 2011; accepted 8 February 2012; published online 23 February 2012)

A comparison between the results of x-ray absorption spectroscopy of runaway electrons (RAEs) generated during nanosecond timescale high-voltage (HV) gas discharge and the simulated attenuation of the x-ray flux produced by the runaway electron spectrum calculated using particle-in-cell numerical modeling of such a type of discharge is presented. The particle-in-cell simulation considered the field and explosive emissions (EEs) of the electrons from the cathode. It is shown that the field emission is the dominant emission mechanism for the short-duration (<2.5 ns) high-voltage pulses, while for the long-duration (>5 ns) high-voltage pulses, the explosive emission is likely to play a significant role. © *2012 American Institute of Physics*. [http://dx.doi.org/10.1063/1.3689010]

Today, nanosecond and sub-nanosecond high-voltage (HV) and high-current electrical discharges in pressurized gas are used in various applications, such as x-ray generation, laser pumping, and gap spark switches.[1] This type of discharge[2–4] is accompanied by the generation of runaway electrons (RAEs), which presumably pre-ionize the gas inside the cathode-anode (CA) gap and lead to the generation of a fast propagating ionization wave.[5,6]

Because of the sub-nanosecond timescale of the discharge, investigation of the RAE generation inside the CA gap with the required time and space resolution is problematic. Today, the parameters of RAE behind the thin anode foil are studied using Faraday cups, collectors, foil spectrometry, and the time-of-flight method.[2–5,7–9] Since the 1960s (see, for instance, Refs. 10–14), the detection and analysis of the x-rays produced by the RAE's interaction with the anode have remained a reliable method of obtaining important data on RAE generation. Nevertheless, none of these diagnostic methods allows one to determine the RAE source(s) inside the CA gap or the phenomena responsible for RAE generation. It was supposed that RAE consist of electrons emitted from the cathode as well as of electrons emitted from the moving boundary of the plasma channel.[3,4,15] In addition, it was suggested,[4] and confirmed by the results of numerical simulations,[16] that the termination of the RAE generation occurs as a result of either the shielding of the electric field that causes the field emission (FE) by the space charge generated inside the CA gap[15,17] or the transformation of FE to explosive emission (EE).[16] It is important to note that the time delay in the EE beginning in gas-filled diodes is still debatable issue (see, for instance, Refs. 4, 18 and 19). The separation between space charges of electrons and ions generated in non-uniform electric field in the cathode vicinity changes drastically the electric field at the cathode surface and, for instance, in Refs. 17 and 18, it was shown that in gas-filled diode, the EE could start at 50 ps with respect to the beginning of the HV pulse.

In this paper, it will be shown that attenuation dependencies of experimentally obtained and simulated x-rays fluxes generated by RAE interaction with the anode can be used to resolve the dominant mechanism responsible for electron emission during the nanosecond HV discharge in pressurized air.

In order to calculate the electron energy distribution function (EEDF) in nanosecond timescale gas discharge, the one dimensional particle-in-cell (1D PIC) numerical code described in detail in Refs. 14 and 15 was used. In simulations, a coaxial diode filled with N_2 gas at pressures of $1–3 \times 10^5$ Pa and with cathode and anode radii of 3 μm and 1 cm, respectively, and a length of 1 cm was considered. In the simulations, N_2 gas (instead of air used in experiment) was considered, since the maximum of inelastic energy losses in both N_2 and O_2 corresponds to almost same energy and cross section. Briefly, the sequence of the 1D PIC simulation was as follows: (a) solution of the Poisson equation at the beginning of each time step for new electron and ion space charge densities and for new boundary conditions: zero anode potential and cathode potential varying in time as $\varphi_c = -\varphi_0 \sin(2\pi \cdot t/T)$, where φ_0 is the maximal cathode potential and $T/4$ is its rise time; (b) calculation of the number of emitted electrons, which is determined by FE according to the Fowler-Nordheim law[20] or by FE transferring into EE (Ref. 1) with a time delay, t_d, which requires zero electric field at the cathode surface; (c) numerical simulation of electron-neutral elastic and inelastic collisions using the Monte-Calro methods with the accounting for forward and backward scattering;[21] and (d) particles weighting on the spatial grid and returning to step (a). The time step of 10^{-14} s allows us to consider electrons propagating only a part of the mean free path during one time step. Here, let us note that the switching from the FE to EE leads to propagation of the cathode emission boundary toward the anode with an ion-sound velocity $V_C = 2 \times 10^4$ m/s.[1] Here, it was supposed that the explosive plasma obtains the cathode potential. In addition, at the time interval, when the EE is switched on, the electrons were emitted uniformly with an initial velocity[1] of 10^6 m/s and added into the numerical cell closest to the

[a]Author to whom correspondence should be addressed. Electronic mail: dima.levko@gmail.com.

cathode. Also, the influence of photoemission process[22] on RAE generation was neglected since the number of electrons emitted as a result of photoemission by photons produced inside CA gap by various processes is much smaller than the number of field emitted electrons from the cathode that become runaway.[23]

In the case when only the FE was considered,[14] the simulation results showed that for an HV pulse with a rise time in the range $T/4 = 0.25$–2 ns, the RAE generation is strongly affected by the space charge distribution of electrons and ions formed inside the CA gap due to gas ionization by RAE and secondary electrons. That is, the separation between electrons and ions at some distance from the cathode at time t_{VC} causes the formation of a virtual cathode (VC). On the one hand, VC terminates the generation of RAE composed of electrons emitted by the cathode and existing in the gap between the cathode and VC. On the other hand, VC becomes a source of RAE if the electric field exceeds a critical value E_{cr} at its anode side (for instance, in N_2 at $P = 10^5$ Pa and $E_{cr} \approx 450$ kV/cm).

When the EE was turned on with a variable time delay t_d with respect to the beginning of the HV pulse, the results of PIC simulations[15] showed that the value of t_d significantly influences the EEDF. Namely, it was shown that if the EE is turned on prior to the VC formation, one obtains screening of the electric field in the cathode vicinity. The latter occurs due to the increased flux of electrons emitted from the boundary of explosive plasma. This terminates the generation of RAE in the vicinity of the cathode.

When EE is turned on after the VC formation and during the HV rise time, the value of t_d does not significantly influence the RAE parameters. That is, the results of simulations showed that at $t_d > t_{VC}$, the VC is a major source of RAE and, therefore, electrons emitted from the explosive plasma do not influence RAE generation.

Let us note that in the case of an HV pulse with $T/4 = 5$ ns, the results of simulations with only FE-emitted electrons showed that the VC is not formed [see Fig. 1(a)] because of the compensation of electron charge by moving N_2^+ ions and slower growth of the cathode potential, which leads to a weaker FE and a lower rate of gas ionization in the cathode vicinity. In this case, it is the turning on of the EE at $t_d = 2.1$ ns that leads to the formation of the VC [see Fig. 1(a)], which becomes the source of RAE.

Figs. 1(b) and 1(c) shows simulated EEDFs obtained at the end of the HV pulse at the anode for the cases when electron emission from the cathode is governed by either FE or FE, which transforms into EE at $t_d = 2.1$ ns for $T/4 = 5$ ns, $\varphi_0 = 160$ kV, and $P = 10^5$ Pa [see Fig. 1(b)] or at $t_d = 160$ ps for $T/4 = 0.5$ ns, $\varphi_0 = 120$ kV, and $P = 10^5$ Pa [see Fig. 1(c)]. One can see a significant difference between these EEDFs, which can be explained by the different potential distribution evolution inside the CA gap. In spite of the fact that in the case of an electron FE and HV pulse with $T/4 = 5$ ns a VC is not formed [see Fig. 1(a)], the generated space charge changes the potential distribution significantly, causing a decrease in the electric field at the cathode surface in comparison with the vacuum case. This leads to a decrease in the number of FE-emitted electrons and, respectively, to a decrease in the number of electrons at the high energy tail of

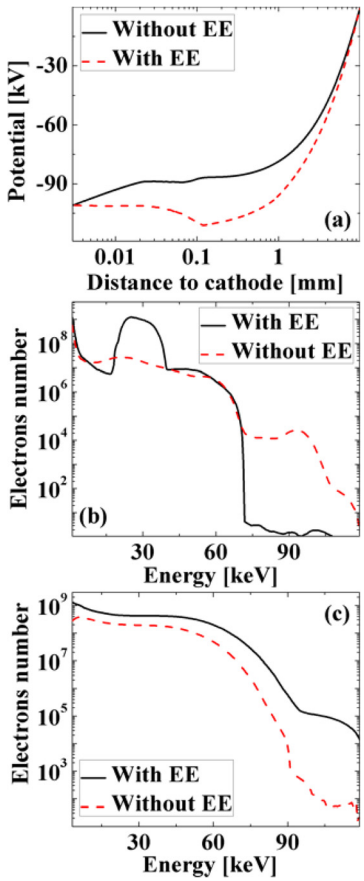

FIG. 1. (Color online) (a) Simulated potential distribution at $t \approx 2.3$ ns (with respect to HV pulse beginning) with and without EE for HV pulse with $T/4 = 5$ ns, $\varphi_0 = 160$ kV, and $P = 10^5$ Pa for $t_d = 2.1$ ns. Comparison between simulated EEDF at the anode with and without EE: (b) $T/4 = 5$ ns, $\varphi_0 = 160$ kV, and $P = 10^5$ Pa at $t_d = 2.1$ ns and (c) $T/4 = 0.5$ ns, $\varphi_0 = 120$ kV, and $P = 10^5$ Pa at $t_d = 160$ ps and $t_{VC} \approx 123$ ps.

the EEDF. For an HV pulse with $T/4 = 5$ ns, when the EE is turned on, one obtains different EEDFs depending on the value of t_d. Namely, for $t_d < T/4$, there is an additional peak in EEDF for electrons with $\varepsilon_e \sim 30$ keV, and the number of electrons with $\varepsilon_e > 70$ keV is greatly reduced [see Fig. 1(b)]. In addition, the simulations showed that the energy of this peak in EEDF depends on the value of t_d. The appearance of this peak can be explained by the additional energy which acquires electrons already existing in the CA gap. The latter occurs due to the increase in the electric field caused by EE-emitted electrons.[15] In the case of the HV pulse with $T/4 = 0.5$ ns, one also obtains a change in the EEDF [see Fig. 1(c)], namely, the turning on of the EE for values $t_d > t_{VC}$ leads to an increase in the number of RAE in the high-energy tail of the EEDF. This effect can be explained also by the sharp increase in the number of the EE-emitted electrons, which increases the VC negative potential and electric field from the anode side of the VC. This leads to an increased number and energy of the electrons emitted from the anode side of the VC and reaching the anode.[15] Thus, the results of our PIC simulations showed that the EEDF of RAE depends on the type of electron emission phenomenon, i.e., either the FE or the EE governs the electron emission from the cathode.

The interaction of electrons with energy ε_e with the anode causes the generation of bremsstrahlung x-ray radiation

in the energy interval $0 \le \varepsilon \le \varepsilon_e$. Therefore, the increase in the number of electrons in the high-energy tail of EEDF, which depends on the type of the electron emission, should lead to an increase in the intensity of the high-energy x-rays and, respectively, to an increase in the x-ray intensity behind a filter of a certain thickness. Thus, a comparison between experimental and simulated x-ray attenuation dependencies could allow one to make a suggestion as to which electron emission phenomenon governs the electron emission during HV nanosecond pulsed discharge in pressurized gases.

The simulated EEDFs with and without EE of electrons were used as input parameters for the computer simulation (really should be just a "computer simulation" otherwise the abbreviation should be explained) described in detail in Ref. 14 for producing x-ray attenuation curves, which were compared with experimental data. These simulations included the electron energy losses in the *Ta* foil using the data on electron stopping power;[24] the generation of x-rays is calculated using the forward bremsstrahlung cross-section.[25] The decay of the simulated x-ray flux in the *Ta* foil and *Al* filters was calculated using the x-ray attenuation coefficients.[24] Taking into account x-ray energy losses in the vinyl-toluene scintillator,[24] the time-integrated flux of these photons behind the *Ta* and *Al* filter was obtained for the different thicknesses of *Al* filter used in the experiment, creating a simulated attenuation curve.

The experimental research of x-ray fluxes produced by RAE interaction with the anode was carried out using a gas-filled diode with a CA gap of variable length (d_{CA}) supplied by high-voltage pulses with durations of 1 ns, 5 ns, and 20 ns full width at half maximum and amplitudes of ~140 kV, ~170 kV, and ~160 kV, respectively, produced by an all-solid state generator.[26] The diode setup used in these experiments is described in detail in Ref. 14.

For x-ray spectrometry, a Saint-Gobain BC408 plastic scintillator was used with *Al* filters in front of it and a photomultiplier tube (PMT) Hamamatsu R7400 placed behind the filters. The obtained time-integrated signal of the PMT represents the relative amount of fluorescent photons. A decay curve of the PMT signal versus the *Al* filters' thickness was obtained for different values of gas pressures and d_{CA}. For each thickness of the *Al* filter, the obtained data point represents the average of around 25 shots and the error bar does not exceed 4%. The intensity behind each *Al* filter was normalized to the intensity behind the 2 mm-thick *Al* plate.

Fig. 2(a) shows the comparison between the results of experiments and simulations for both models, i.e., with and without EE of electrons, for HV pulses with $T/4 = 0.5$ ns and maximum amplitude of 120 kV. One can see that, in general, all four simulated x-ray attenuation curves can be used for fitting of the experimental data. However, the best fit is achieved when only FE is taken into account or for the cases when the EE is turned on at $t_d < 120$ ps. Also, one can see that the increase in the value of t_d increases the x-rays' intensity at a greater thickness of the *Al* foil (i.e., the increase in the number of electrons in the high-energy tail of EEDF [see Fig. 1(c)]) leading to larger deviation from the experimental curve. Here, let us note that the EE could be considered only when the specific action integral[1] $j^2 t_d \approx h$ reaches some critical value of 1.4×10^9 $A^2 \cdot s \cdot cm^{-4}$ for iron that requires the current density $j \approx 4 \times 10^{10}$ A/cm^2 for $t_d = 120$ ps, which can hardly be obtained in experiments. Thus, one can suggest that at short (~1 ns) duration HV pulses with amplitude of $\sim 1.5 \times 10^5$ V, the most probable RAE source is FE.

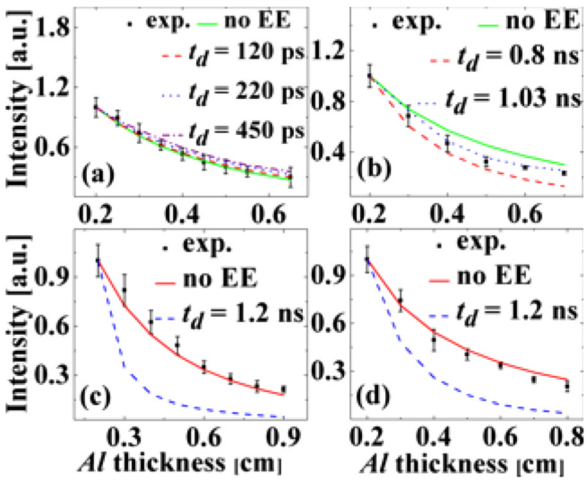

FIG. 2. (Color online) Comparison of simulated and experimental x-ray attenuation curves at different times of the beginning of the EE of electrons: (a) $T/4 = 0.5$ ns, $\varphi_0 = 120$ kV, and $P = 10^5$ Pa; (b) $T/4 = 5$ ns, $\varphi_0 = 160$ kV, and $P = 10^5$ Pa; (c) $T/4 = 2.5$ ns, $\varphi_0 = 160$ kV, and $P = 2.3 \times 10^5$ Pa; (d) $T/4 = 2.5$ ns, $\varphi_0 = 160$ kV, and $P = 3 \times 10^5$ Pa.

In the case of an HV pulse with $T/4 = 5$ ns, the VC is not formed and the turning on the EE of electrons decreases the number of electrons in the high-energy tail of EEDF. The latter decreases the intensity of x-rays due to the greater thicknesses of *Al* foil. Fig. 2(b) demonstrates that the best fit between experimental and simulated x-ray attenuation curves is obtained when the EE of electrons was turned on at $t_d = 1.03$ ns; noticeable deviation from the experiment is obtained with $t_d < 1.03$ ns or for the case of FE only. Thus, one can suppose that the EE occurs with the time delay $t_d \sim 1$ ns in HV gaseous discharges with voltage amplitude of $\sim 1.5 \times 10^5$ V and time duration of ~10 ns and significantly contributes to the number of high-energy RAE.

The results of the application of the proposed method for the gas discharge at pressures of 2.3×10^5 Pa and 3×10^5 Pa and HV pulse with $T/4 = 2.5$ ns and $\varphi_0 = 160$ kV are shown in Figs. 2(c) and 2(d). One can see that the best fit between the experimentally and simulated x-ray attenuation curves was obtained when only FE was considered. In these simulations, the EE turns on at $t_d = 1.2$ ns. A decrease in the value of t_d leads to an increase in the deviation between the simulated and experimentally obtained x-ray attenuation curves. From the discussion presented above, one could conclude that the increase in the value of t_d should cause an increase in the number of electrons in the high-energy tail of EEDF and, respectively, better agreement with the experimental data. However, the results of the simulations showed that at the considered pressure values, the space charge of electrons emitted by FE significantly screens the electric field at the cathode emitting surface and the VC already forms at $t \approx 1.2$ ns. Thus, it is not reasonable to consider turn-on of the FE at $t > 1.2$ ns.

To conclude, it was shown that the comparison between experimentally and simulated x-rays attenuation curves can be used to determine the dominant mechanism responsible

for electron emission during the nanosecond HV discharge in pressurized air. Namely, for HV pulses with the rise times in the range 0.5-2.5 ns and amplitudes of $\sim 1.5 \cdot 10^5$ V, the dominant mechanism of electron emission is FE and for longer duration HV pulses, one has to account for the EE of electrons as well.

This work was supported in part by a fellowship from the Lady Davis Foundation and the Technion Grant No. 2013371.

[1]G. A. Mesyats, *Pulsed Power and Electronics* (Nauka, Moscow, 2004) (in Russian).
[2]L. P. Babich, T. V. Loiko, V. A. Tsukerman, Phys. Usp. **33**, 521 (1990) and references therein.
[3]V. F. Tarasenko, S. I. Yakovlenko, Phys. Usp. **47**, 887 (2004) and references therein.
[4]G. A. Mesyats, M. I. Yalandin, K. A. Sharypov, V. G. Shpak, and S. A. Shunailov, IEEE Trans. Plasma Sci. **36**, 2497 (2008).
[5]L. M. Vasilyak, S. V. Kostyuchenko, N. N. Kudryavtsev, and I. V. Filyugin, Phys. Usp. **27**, 247 (1994) and references therein.
[6]S. M. Starikovskaia and A. Yu. Starikovskii, J. Phys. D: Appl. Phys. **34**, 3391 (2001).
[7]V. F. Tarasenko and S. I. Yakovlenko, Plasma Devices Oper. **13**, 231 (2005).
[8]T. Shao, Ch. Zhang, Zh. Niu, P. Yan, V. F. Tarasenko, E. Kh. Baksht, A. G. Burahenko, and Y. V. Shut'ko, Appl. Phys. Lett. **98**, 021503 (2011).
[9]V. F. Tarasenko, Plasma Phys. Rep. **37**, 409 (2011).
[10]S. Frankel, V. Highland, T. Sloan, O. van Dyck, and W. Wales, Nucl. Instrum. Methods **44**, 345 (1966).
[11]Yu. L. Stankevich and V. G. Kalinin, Sov. Phys. Dokl. **12**, 1042 (1967).
[12]R. C. Noggle, E. P. Krider, and J. R. Wayland, J. Appl. Phys. **39**, 4746 (1968).
[13]L. P. Babich, *High-Energy Phenomena in Electric Discharges* (Futurepast, Virginia, 2003).
[14]S. Yatom, V. Vekselman, J. Z. Gleizer, and Ya. E. Krasik, J. Appl. Phys. **109**, 073312 (2011).
[15]D. Levko, S. Yatom, V. Vekselman, J. Z. Gleizer, V. Tz. Gurovich, and Ya. E. Krasik, J. Appl. Phys. **111**, 013303 (2012).
[16]D. Levko, S. Yatom, V. Vekselman, J. Z. Gleizer, V. Tz. Gurovich, and Ya. E. Krasik, J. Appl. Phys. **111**, 013304 (2012).
[17]S. Ya. Belomyttsev, I. V. Romanchenko, V. V. Ryzhov, and V. A. Shklyaev, Tech. Phys. Lett. **34**, 367 (2008).
[18]S. N. Ivanov, Dokl. Phys. **49**, 701 (2004).
[19]J. E. Chaparro, "Investigation of sub-nanosecond breakdown through experimental and computational methods," Ph. D. dissertation (Texas Tech University, 2008).
[20]Yu. P. Raizer, *Gas Discharge Physics* (Springer, Berlin, 1991).
[21]Y. Itikawa, J. Phys. Chem. Ref. Data **35**, 31 (2006).
[22]A. P. Bokhan, P. A. Bokhan, and D. E. Zakrevsky, Appl. Phys. Lett. **86**, 151503 (2005).
[23]D. Levko, V. Tz. Gurovich, and Ya. E. Krasik, J. Appl. Phys. **111**, 013306 (2012).
[24]J. H. Hubbel and S. M. Seltzer, "Tables of x-ray mass attenuation coefficients and mass energy-absorption coefficients from 1 keV to 20 MeV for elements Z = 1 to 92 and 48 additional substances of dosimetric interest," NIST Physical Reference Data.
[25]G. E. Desorby and A. L. Boyer, Med. Phys. **18**, 497 (1990).
[26]S. N. Rukin, Instrum. Exp. Tech. **42**, 439 (1999).